Journal of Fluids and Structures (2000) **14,** 235–255
doi: 10.1006/jfls. 1999.0267, available online at http://www.idealibrary.com on IDEAL®

VIBRATIONS OF FLUID-FILLED HERMETIC CANS

M. AMABILI

Department of Industrial Engineering, University of Parma, Parco Area delle Scienze 181/A Parma, 43100, Italy

(Received 3 February 1999, and in final form 21 September 1999)

Free, conservative vibrations of a hermetic can, simply supported at the base, are studied. The can is composed by a circular cylindrical shell and two identical circular plates connected to the shell at its ends. The artificial spring method, which is an extension of the classical Rayleigh–Ritz method, is used to solve the system by using substructuring. The can is studied empty and filled with an inviscid and incompressible fluid. Fluid volume conservation is applied. The interaction between the plates and the shell via the fluid is considered, and exact expressions for the fluid velocity potential are used. The effect of flexibility of joints between plates and shell is investigated. Results for a fluid-filled, simply supported shell closed by rigid ends are also obtained and compared to the classical open-end shell.

1. INTRODUCTION

HERMETIC CANS ARE LARGELY EMPLOYED as containers of liquids. They are composed of a circular cylindrical shell, joined to two circular end-plates. Their modal behaviour has been investigated in the empty case by several researchers. Hirano (1969) studied axisymmetric vibrations of thin drums (cans) by minimizing the Lagrangian; this approach was extended to other modes by Takahashi and Hirano (1970). Takavoli & Singh (1989, 1990) studied theoretically a hermetic can by using the state-space method, which is a transfer-matrix-based substructuring method; they also investigated the same can experimentally and by using a FEM code. Huang & Soedel (1993) applied the receptance method to the study of free vibrations of circular plates welded to a cylindrical shell, including the hermetic can case. A similar problem has been investigated by Yuan & Dickinson (1994) by using the artificial spring method which is an extension of the classical Rayleigh–Ritz method, suitable for substructuring. This method had been developed by Yuan and Dickinson (1992) and Cheng & Nicolas (1992). The artificial spring method has been extended to study fluid–structure interaction by Cheng (1994) in the case of a light-fluid approximation and by Amabili (1997a, b) in the case of dense fluid (liquid).

The only work related to vibrations of cans in contact with dense fluid is that of Harari *et al.* (1994), studying a stiffened and submerged cylindrical shell closed by two end-plates and immersed in unbounded fluid. They neglected the interaction between the plates and the shell via the fluid and used the expression of the fluid load on the end-plates obtained for circular plates with a rigid extension (circular plate in an infinite baffle). No studies are available for free vibrations of liquid-filled cans. Otherwise, liquid-filled tanks composed of a circular cylindrical shell and a flexible or rigid bottom plate have been widely studied, e.g. by Amabili *et al.* (1998), Amabili (1997a), Chiba (1996), Gonçalves & Ramos (1996), Yamaki *et al.* (1984); however, in these studies there exists a free liquid surface and hence they are only partially related to the present case.

0889–9746/00/020235 + 21 $35.00/0

The present study investigates free, conservative vibrations of a hermetic can, simply supported at the base. The can is composed of a circular cylindrical shell and two identical circular plates connected to the shell at its ends. The use of artificial springs at the junctions allows us to study vibrations of this relatively complex system. In particular, the joints between the components of the structure are replaced by artificial springs that are distributed along the entire joint length. Only rotation at the shell–plate joints is coupled by rotational springs. The can is first studied empty and then filled with an inviscid and incompressible fluid. Fluid volume conservation is applied. The interaction between the plates and the shell via the fluid is considered and exact expressions of the fluid velocity potential are used. The effect of flexibility of joints between plates and shell is also investigated.

2. THE EMPTY CAN

The system studied is composed of a circular cylindrical shell and two circular plates connected to the shell at its ends. The bottom plate is assumed to be simply supported, in order to prevent rigid-body modes of the system. When a plate is joined to a circular cylindrical shell, in general three displacements and two slope connections could be considered, according to classical thin shell theory. However, if one only investigates lower modes of the system, the plates can be assumed inelastic in their plane. Moreover, influences of connection deflections in the tangential planes of the shell can be neglected with respect to transverse amplitudes. Actually, for very thick plates, the shell axial constraint can be important and it should be properly modelled, but this is very limited for thin plates. Therefore, only the radial slope at the plate boundary can be considered to be coupled to the axial slope of the shell at the ends. A similar approach was used by Cheng & Nicolas (1992), Cheng (1994), Amabili (1997a) and Amabili *et al.* (1998). Huang & Soedel (1993) used two connections when the plate was not connected to the shell simple support. In the present case, only one connection is used. In fact, the joints between the shell and the plates give a reciprocal constraint that can be modelled as a simple support. Therefore, their reciprocal rotation at the edges is joined by introducing artificial rotational springs of appropriate stiffness. The stiffnesses of these springs are chosen to be very high with respect to the stiffness of the flexible components of the can, in order to simulate a welded connection between the shell and the plates. Moreover, the effect of the elasticity of the joint is investigated by using the present model.

The top plate gives to the top end of the shell a constraint that can be conveniently modelled with a simple support for all the modes of vibration without movement of the can longitudinal axis. On the other hand, for beam-bending modes of the can, the cross-section of the shell at the top end remains circular but it moves with respect to the base, so that the top plate does not constrain these modes. Hence, these modes may correctly be studied by considering a free top-end of the shell component. In the present study, the shell is considered to be simply supported at both ends, so that this model cannot be used to study the beam-bending modes of cans simply supported only at the base. However, for the usual geometry of cans, lower shell-modes present more than one circumferential wave and can be conveniently studied by using the present model.

The hermetic can considered has radius a and height L, and is conveniently studied in the polar coordinates (x, r, θ); the origin O of the coordinate system is placed on the can axis at half-distance from the end-plates (Figure 1). Due to the axial symmetry of the structure, only modes of the shell and the plates with the same number n of nodal diameters (or circumferential waves) are coupled. A nodal diameter is a diameter in the cross-section of the shell (or in the plane of the plate) connecting points which are immobile during vibration.

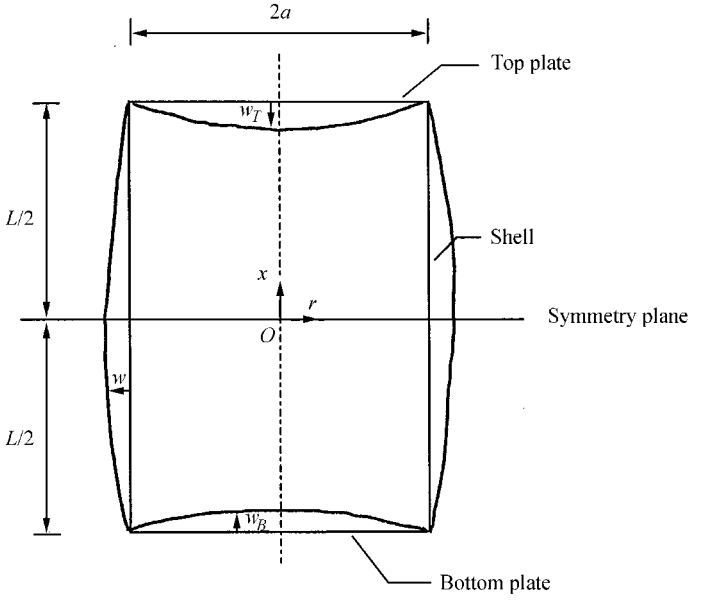

Figure 1. Geometry of the can and coordinate system.

Besides, it is interesting to note that, due to axial symmetry, for each asymmetric mode ($n > 0$) there exists a second mode having the same frequency and shape but angularly rotated by $\pi/2n$.

In the present study identical end-plates are considered, so that the system is symmetric with respect to the plane $x = 0$; therefore, it displays only symmetric and antisymmetric modes, in a radial section of the can, with respect to this plane.

The Rayleigh–Ritz method (Amabili 1997b) is applied to find natural frequencies and modes of the fluid-filled can, the time variation being assumed to be harmonic. Therefore, the mode shapes w of the shell wall in the radial direction (Figure 1) can be expressed as follows:

$$w(x,\theta) = \begin{cases} \cos(n\theta) \sum_{s=1}^{\infty} q_s \cos[(2s-1)\pi x/L] & \text{symmetric modes} \\ \cos(n\theta) \sum_{s=1}^{\infty} q_s \sin(2s\pi x/L) & \text{antisymmetric modes,} \end{cases} \tag{1}$$

where n and s are the number of nodal diameters and of axial half-waves, respectively, and q_s are the parameters of the Ritz expansion. The eigenvectors of the empty simply supported cylindrical shell are used as admissible functions.

The mode shapes w_B of the bottom circular plate in the transverse direction of the plate can be given as (Amabili 1997a)

$$w_B(r,\theta) = \cos(n\theta) \sum_{i=0}^{\infty} b_i [A_{n,i} \mathrm{J}_n(\lambda_{n,i} r/a) + C_{n,i} [\mathrm{I}_n(\lambda_{n,i} r/a)], \tag{2}$$

where n and i are the number of nodal diameters and circles, respectively, a is the plate radius, b_i are the parameters of the Ritz expansion, and $\lambda_{n,i}$ is the well-known frequency parameter that is related to the plate natural frequency; J_n and I_n are the Bessel function and

modified Bessel function of order n, respectively. In equation (2), the *in vacuo* eigenfunctions of the simply supported circular plate are assumed as admissible functions. The trial functions are linearly independent and constitute a complete set. Values of $\lambda_{n,i}$ for simply supported plates are given, e.g., by Leissa & Narita (1980).

Similarly, mode shapes w_T of the top circular plate can be given as

$$w_T(r,\theta) = \cos(n\theta) \sum_{i=0}^{\infty} h_i [A_{n,i} \mathrm{J}_n(\lambda_{n,i} r/a) + C_{n,i} \mathrm{I}_n(\lambda_{n,i} r/a)], \tag{3}$$

where h_i are the parameters of the Ritz expansion. To simplify the computations, the mode shape constants, $A_{n,i}$ and $C_{n,i}$, are normalized in order to have (Wheelon 1968)

$$\begin{aligned} &\int_0^1 [A_{n,i}\mathrm{J}_n(\lambda_{n,i}\rho) + C_{n,i}\mathrm{I}_n(\lambda_{n,i}\rho)]^2 \rho \,\mathrm{d}\rho \\ &= \left\{ \frac{A_{n,i}^2}{2} \left[(\mathrm{J}_n'(\lambda_{n,i}))^2 + \left(1 - \frac{n^2}{\lambda_{n,i}^2}\right) \mathrm{J}_n^2(\lambda_{n,i}) \right] - \frac{C_{n,i}^2}{2} \left[(\mathrm{I}_n'(\lambda_{n,i}))^2 - \left(1 + \frac{n^2}{\lambda_{n,i}^2}\right) \mathrm{I}_n^2(\lambda_{n,i}) \right] \right. \\ &\left. + \frac{A_{n,i} C_{n,i}}{\lambda_{n,i}} [\mathrm{J}_n(\lambda_{n,i}) \mathrm{I}_{n+1}(\lambda_{n,i}) + \mathrm{I}_n(\lambda_{n,i}) \mathrm{J}_{n+1}(\lambda_{n,i})] \right\} = 1, \end{aligned} \tag{4}$$

where $\rho = r/a$ and J_n' and I_n' indicate the derivatives of J_n and I_n with respect to the argument. The ratio of the mode shape constants for simply supported plates is

$$A_{n,i}/C_{n,i} = -\mathrm{I}_n(\lambda_{n,i})/\mathrm{J}_n(\lambda_{n,i}). \tag{5}$$

It is interesting to note that, for the system of Figure 1, the following conditions can be imposed:

$$w_T = w_B \quad \text{symmetric}; \qquad w_T = -w_B \quad \text{antisymmetric modes}. \tag{6a, b}$$

By using equations (6) we get

$$h_i = b_i \quad \text{symmetric}; \qquad h_i = -b_i \quad \text{antisymmetric modes}. \tag{7a, b}$$

In order to solve the problem, we evaluate the kinetic and potential energies of the shell, plates and fluid. The reference kinetic energy T_S^* of the shell, neglecting the tangential and rotary inertia, is given by

$$T_S^* = \frac{1}{2} \rho_S h_S \int_0^{2\pi} \int_{-L/2}^{L/2} w^2 \mathrm{d}x \, a \, \mathrm{d}\theta = \frac{1}{2} \rho_S h_S a (L/2) \psi_n \sum_{s=1}^{\infty} q_s^2, \tag{8}$$

where h_S is the shell thickness, ρ_s is the density of the shell material (kg/m^3) and

$$\psi_n = \begin{cases} 2\pi & \text{for } n = 0 \\ \pi & \text{for } n > 0 \end{cases}.$$

In equation (8) the orthogonality of the sine function in the interval $[-L/2, L/2]$ has been used. Similarly, the reference kinetic energy T_p^* of the plates is given by

$$T_P^* = \frac{1}{2} \rho_P h_P \int_0^{2\pi} \int_0^a (w_B^2 + w_T^2) r \, \mathrm{d}r \, \mathrm{d}\theta = \rho_P h_P a^2 \psi_n \sum_{i=0}^{\infty} b_i^2, \tag{9}$$

where h_P is the plate thickness and ρ_P is the density of the plate material (kg/m^3). In equation (9) the orthogonality of Bessel functions (plate mode shapes) in $[0, a]$ has been used.

It should be noted that the maximum potential energy of each mode of the empty shell (without the end plates) is equal to the reference kinetic energy of the same mode multiplied by the squared circular frequency $\omega_s{}^2$ of this mode. Moreover, due to the series expansion of the mode shape, the potential energy is the sum of the energies of each single component mode. As a consequence, the maximum potential energy of the shell may be expressed as

$$V_S = \tfrac{1}{2}\rho_S h_S a(L/2)\psi_n \sum_{s=1}^{\infty} q_s^2 \omega_s^2, \tag{10}$$

where ω_s are the circular frequencies of the symmetric and antisymmetric flexural modes of the simply supported shell that can be computed by using, for example, the Flügge theory of shells (Leissa 1973). Similarly, the maximum potential energy of the two end-plates is the sum of the reference kinetic energies of the eigenfunctions of the plates in vacuum multiplied by $\tilde{\omega}_{n,i}^2$:

$$V_P = \rho_P h_P a^2 \psi_n \sum_{i=0}^{\infty} b_i^2 \tilde{\omega}_{n,i}^2 = \frac{D}{a^2}\psi_n \sum_{i=0}^{\infty} b_i^2 \lambda_{n,i}^4, \tag{11}$$

where the plate circular frequency $\tilde{\omega}_{n,i}^2$ is related to the frequency parameter $\lambda_{n,i}$ by $\tilde{\omega}_{n,i} = (\lambda_{n,i}^2/a^2)[D/(\rho_P h_P)]^{1/2}$ and $D = E_P h_P^3/[12(1-v_P^2)]$ is the flexural rigidity of the plates; v_P and E_P are the Poisson ratio and Young's modulus of the plates, respectively.

In a can section containing the can axis, the rotations at the plate edges are considered joined to the rotations at the shell edges, as previously discussed. The shell and the plates are connected together by artificial rotational springs of appropriate stiffness, continuously distributed around the circumference.

The maximum potential energy of the two distributed rotational springs connecting the two end-plates and the shell is

$$V_C = \frac{1}{2}\int_0^{2\pi} c\left\{\left[\left(\frac{\partial w}{\partial x}\right)_{x=-L/2} + \left(\frac{\partial w_B}{\partial r}\right)_{r=a}\right]^2 + \left[\left(\frac{\partial w}{\partial x}\right)_{x=L/2} - \left(\frac{\partial w_T}{\partial r}\right)_{r=a}\right]^2\right\} a\,\mathrm{d}\theta, \tag{12}$$

where c is the spring stiffness (N m/m). It should be noted that only the variation of the angle between the shell and the plates contributes to the potential energy stored by the rotational spring. Simple calculations for symmetric modes give

$$V_C = ca\psi_n\left\{\frac{\pi^2}{L^2}\sum_{s=1}^{\infty}\sum_{j=1}^{\infty} q_s q_j(-1)^s(-1)^j(2s-1)(2j-1) + \sum_{i=0}^{\infty}\sum_{h=0}^{\infty} b_i b_h \frac{\lambda_{n,i}}{a}\frac{\lambda_{n,h}}{a}\right.$$

$$\times[A_{n,i}\mathrm{J}'_{\mathrm{n}}(\lambda_{n,i}) + C_{n,i}\mathrm{I}'_{\mathrm{n}}(\lambda_{n,i})]\times[A_{n,h}\mathrm{J}'_{\mathrm{n}}(\lambda_{n,h}) + C_{n,h}\mathrm{I}'_{\mathrm{n}}(\lambda_{n,h})]$$

$$\left. - 2\frac{\pi}{L}\sum_{s=1}^{\infty}\sum_{i=0}^{\infty} q_s b_i(-1)^s(2s-1)\frac{\lambda_{n,i}}{a}[A_{n,i}\mathrm{J}'_{\mathrm{n}}(\lambda_{n,i}) + C_{n,i}\mathrm{I}'_{\mathrm{n}}(\lambda_{n,i})]\right\}, \tag{13a}$$

and for antisymmetric modes

$$V_C = ca\psi_n\left\{\frac{4\pi^2}{L^2}\sum_{s=1}^{\infty}\sum_{j=1}^{\infty} q_s q_j(-1)^s(-1)^j sj + \sum_{i=0}^{\infty}\sum_{h=0}^{\infty} b_i b_h \frac{\lambda_{n,i}}{a}\frac{\lambda_{n,h}}{a}[A_{n,i}\mathrm{J}'_{\mathrm{n}}(\lambda_{n,i}) + C_{n,i}\mathrm{I}'_{\mathrm{n}}(\lambda_{n,i})]\right.$$

$$\left.\times[A_{n,h}\mathrm{J}'_n(\lambda_{n,h}) + C_{n,h}\mathrm{I}'_n(\lambda_{n,h})] + \frac{4\pi}{L}\sum_{s=1}^{\infty}\sum_{i=0}^{\infty} q_s b_i(-1)^s s\frac{\lambda_{n,i}}{a}[A_{n,i}\mathrm{J}'_n(\lambda_{n,i}) + C_{n,i}\mathrm{I}'_n(\lambda_{n,i})]\right\}. \tag{13b}$$

3. DYNAMIC BEHAVIOUR OF THE FLUID-STRUCTURE INTERACTION

The can is considered completely filled with an inviscid and incompressible fluid. Hydrostatic pressure effects and damping are neglected in the present study. For an incompressible and inviscid fluid, the deformation potential satisfies the Laplace equation

$$\nabla^2\phi(r, \theta, x) = 0. \tag{14}$$

The deformation potential ϕ is related to the fluid velocity potential $\tilde{\phi}$ by

$$\tilde{\phi}(x, \theta, r, t) = \mathrm{i}\omega\phi\mathrm{e}^{\mathrm{i}\omega t}, \tag{15}$$

which is assumed to be harmonic; i is the imaginary unit and ω is the natural circular frequency of vibration. The velocity of the fluid $\mathbf{v}$ is related to $\tilde{\phi}$ by $\mathbf{v} = -\operatorname{grad}\tilde{\phi}$. The fluid deformation potential, using the principle of superposition, can be divided into

$$\phi = \phi^{(1)} + \phi^{(2)}, \tag{16}$$

where $\phi^{(1)}$ describes the velocity potential of the fluid associated with the flexible shell while considering the plates as rigid, and $\phi^{(2)}$ describes the fluid velocity potential for the flexible plates while considering the shell as rigid. The boundary conditions imposed to the fluid for the two complementary boundary value problems are (Amabili 1997b)

$$\left(\frac{\partial\phi^{(1)}}{\partial x}\right)_{x=\pm L/2} = 0, \quad \left(\frac{\partial\phi^{(1)}}{\partial r}\right)_{r=a} = -w(x, \theta), \tag{17a, b}$$

$$\left(\frac{\partial\phi^{(2)}}{\partial x}\right)_{x=-L/2} = -w_B(r, \theta), \qquad \left(\frac{\partial\phi^{(2)}}{\partial x}\right)_{x=L/2} = w_T(r,\theta), \quad \left(\frac{\partial\phi^{(2)}}{\partial r}\right)_{r=a} = 0. \tag{18a–c}$$

Equations (17) and (18) express the contact condition between a fluid (without cavitation) and a flexible or rigid wall. The reference kinetic energy T_F^* of the fluid, by using the Greens theorem (e.g. Amabili 1997b), is

$$\begin{aligned} T_F^* &= \frac{1}{2}\rho_F \iint_{S_S+S_B+S_T} \phi\frac{\partial\phi}{\partial z}\,\mathrm{d}S = \frac{1}{2}\rho_F\iint_{S_S}\phi\frac{\partial\phi}{\partial r}\,\mathrm{d}S - \frac{1}{2}\rho_F\iint_{S_B}\phi\frac{\partial\phi}{\partial x}\,\mathrm{d}S + \frac{1}{2}\rho_F\iint_{S_T}\phi\frac{\partial\phi}{\partial x}\,\mathrm{d}S \\ &= -\frac{1}{2}\rho_F\iint_{S_S}(\phi^{(1)}+\phi^{(2)})\,w\,\mathrm{d}S + \frac{1}{2}\rho_F\iint_{S_B+S_T}(\phi^{(1)}+\phi^{(2)})\,w_P\,\mathrm{d}S \\ &= T_{F_1}^* + T_{F_{1-2}}^* + T_{F_{2-1}}^* + T_{F_2}^*, \end{aligned} \tag{19}$$

where ρ_F is the mass density of the fluid, w_P indicates w_B when integrating on S_B and w_T when integrating on S_T, z is the direction normal at any point on the boundary surface of the liquid domain and is pointed outwards, S_S is the shell lateral surface, S_B is the bottom plate surface and S_T is the surface of the top plate.

3.1. Fluid-Shell Interaction

In this section, the fluid–structure interaction of a simply supported, circular cylindrical and flexible shell of a can with rigid end-plates is considered. A large number of papers on the vibrations of partially fluid-filled shells have been published [*e.g.* Berry & Reissner (1958), Lakis & Païdoussis (1971), Bauer & Siekmann (1971), Yamaki *et al.* (1984), Amabili & Dalpiaz (1995), Gonçalves & Ramos (1996), and Chiba (1996)].

The liquid deformation potential $\phi^{(1)}$ is assumed to be of the form (Amabili 1997a)

$$\phi^{(1)} = \sum_{s=1}^{\infty} q_s \Phi_s^{(1)}. \tag{20}$$

The functions $\Phi_s^{(1)}$ are given by

$$\Phi_s^{(1)}(x,r,\theta) = \begin{cases} \cos(n\theta)\left[A_{n,s,0} r^n + \sum_{m=1}^{\infty} A_{n,s,m} \mathrm{I_n}(2m\pi r/L)\cos(2m\pi x/L)\right] & \text{symmetric,} \\ \cos(n\theta) \sum_{m=1}^{\infty} A_{n,s,m} \mathrm{I_n}((2m-1)\pi r/L)\sin((2m-1)\pi x/L) & \text{antisymmetric,} \end{cases} \tag{21}$$

where $A_{n,s,m}$ are coefficients depending on the integers n, s and m. For $n = 0$, $A_{\mathrm{n,s,0}}$ will be assumed to be zero, because two different terms must be added to the deformation potential ϕ, as will be discussed in Section 3.4. The functions $\Phi_s^{(1)}$ satisfy the Laplace equation and the two boundary conditions given in equations (17a); the condition given in equation (17b) is used to compute the coefficients $A_{n,s,m}$. Different solutions are obtained for symmetric and antisymmetric modes. For symmetric modes, equation (17b) gives

$$A_{n,s,0}\, n a^{n-1} + \sum_{m=1}^{\infty} A_{n,s,m} \frac{2m\pi}{L} \mathrm{I}'_n(2m\pi a/L)\cos(2m\pi x/L) = -\cos((2s-1)\pi x/L). \tag{22}$$

Equation (22) must be satisfied for all values $-L/2 \le x \le L/2$. If this equation is multiplied by $\cos(2\pi j x/L)$ and then integrated between $-L/2$ and $L/2$, using the well-known orthogonality properties of the trigonometric functions, the equation becomes

$$\Phi_s^{(1)} = -\frac{1}{\pi}\cos(n\theta)\left[\frac{-2(-1)^s}{(2s-1)na^{n-1}} r^n + \sum_{m=1}^{\infty} \frac{\sigma_{s,m}^{(S)}}{m} \frac{\mathrm{I}_n(2m\pi r/L)}{\mathrm{I}_n(2m\pi a/L)} \cos(2m\pi x/L)\right], \tag{23}$$

where

$$\sigma_{s,m}^{(S)} = \int_{-L/2}^{L/2} \cos(2m\pi x/L)\cos((2s-1)\pi x/L)\,\mathrm{d}x = \frac{L}{\pi}\left[\frac{(-1)^{m-s}}{1+2m-2s} - \frac{(-1)^{m+s}}{-1+2m+2s}\right]. \tag{24}$$

Therefore, the reference kinetic energy $T_{F_1}^*$ of the fluid associated with symmetric modes of the shell is

$$T_{F_1}^* = -\frac{1}{2}\rho_F \int_0^{2\pi}\int_{-L/2}^{L/2} (\phi^{(1)})_{r=a}\, wa\,\mathrm{d}x\,\mathrm{d}\theta$$

$$= \frac{a}{2\pi}\psi_n \rho_F \sum_{s=1}^{\infty}\sum_{j=1}^{\infty} q_s q_j \left[\frac{4(-1)^s(-1)^j aL}{(2s-1)(2j-1)n\pi} + \sum_{m=1}^{\infty} \frac{\sigma_{s,m}^{(S)}\sigma_{j,m}^{(S)}}{m} \frac{\mathrm{I}_n(2m\pi a/L)}{\mathrm{I}_n(2m\pi a/L)}\right]. \tag{25}$$

For antisymmetric modes, equation (17b) gives

$$\sum_{m=1}^{\infty} A_{n,s,m} \frac{(2m-1)\pi}{L} \mathrm{I}'_n((2m-1)\pi a/L)\sin((2m-1)\pi x/L) = -\sin(2s\pi x/L). \tag{26}$$

Similar to the symmetric case, it gives

$$\Phi_s^{(1)} = -\frac{2}{\pi}\cos(n\theta) \sum_{m=1}^{\infty} \frac{\sigma_{s,m}^{(A)}}{2m-1} \frac{\mathrm{I}_n((2m-1)\pi r/L)}{\mathrm{I}'_n((2m-1)\pi a/L)} \sin((2m-1)\pi x/L), \tag{27}$$

where

$$\sigma_{sm}^{(A)} = \int_{-L/2}^{L/2} \sin((2m-1)\pi x/L)\sin(2s\pi x/L)\,\mathrm{d}x = \frac{L}{\pi}\left[-\frac{(-1)^{m-s}}{-1+2m-2s} + \frac{(-1)^{m+s}}{-1+2m+2s}\right]. \tag{28}$$

Therefore, the reference kinetic energy $T_{F_1}^*$ of the fluid associated with antisymmetric modes of the shell is

$$T_{F_1}^* = \frac{a}{\pi}\psi_n \rho_F \sum_{s=1}^{\infty}\sum_{j=1}^{\infty} q_s q_j \sum_{m=1}^{\infty} \frac{\sigma_{sm}^{(A)}\sigma_{jm}^{(A)}\,\mathrm{I}_n((2m-1)\pi a/L)}{(2m-1)\mathrm{I}_n'((2m-1)\pi a/L)}. \tag{29}$$

3.2. Fluid-Plate Interaction

In this section, the fluid–structure interaction of the simply supported, flexible end-plates of a can with a rigid shell is considered. Flexible bottom plates in rigid tanks were studied, e.g., by Bhuta and Koval (1964), Bauer and Siekmann (1971), Chiba (1993) and Amabili (1997c); Bauer (1995) studied the vibration of a circular top plate in a liquid-filled rigid container.

The liquid deformation potential $\phi^{(2)}$ is assumed of the form (Amabili 1997c)

$$\phi^{(2)} = \sum_{i=0}^{\infty} b_i \Phi_i^{(2)}. \tag{30}$$

The functions $\Phi_i^{(2)}$, for symmetric modes, are expressed as

$$\Phi_i^{(2)}(x, r, \theta) = \cos(n\theta) \sum_{k=1}^{\infty} K_{n,i,k}\,\mathrm{J}_n(\varepsilon_{n,k} r/a)\cosh(\varepsilon_{n,k} x/a), \tag{31}$$

where $\varepsilon_{n,k}$ are solutions of the following equation:

$$\mathrm{J}_n'(\varepsilon_{n,k}) = 0,\ k = 1, \ldots, \infty, \tag{32}$$

rejecting the first solution $\varepsilon_{n,k}$ for $n = 0$. The functions $\Phi_i^{(2)}$ satisfy equations (14) and (18c). The constants $K_{n,i,k}$ are calculated in order to satisfy equations (18a, b)

$$\sum_{k=1}^{\infty} K_{n,i,k}\,\mathrm{J}_n(\varepsilon_{n,k} r/a)(\varepsilon_{n,k}/a)\sinh(\varepsilon_{n,k} L/(2a)) = [A_{n,i}\mathrm{J}_n(\lambda_{n,i} r/a) + C_{n,i}\mathrm{I}_n(\lambda_{n,i} r/a)]. \tag{33}$$

Equation (33) must be satisfied for all values $0 \le r \le a$. If this equation is multiplied by $(1/a^2)\mathrm{J}_n(\varepsilon_{n,k} r/a) r$ and integrated between 0 and a, then using the orthogonality of the Bessel functions this becomes

$$K_{n,i,k} = \frac{a(A_{n,i}\beta_{n,i,k} + C_{n,i}\gamma_{n,i,k})}{(\alpha_{n,k}\varepsilon_{n,k})\sinh(\varepsilon_{n,k} L/(2a))}, \tag{34}$$

where, by using equation (32), one obtains (Wheelon 1968)

$$\alpha_{n,k} = \frac{1}{a^2}\int_0^a \mathrm{J}_n^2(\varepsilon_{n,k} r/a) r\,\mathrm{d}r = \frac{1}{2}\left[1 - \left(\frac{n}{\varepsilon_{n,k}}\right)^2\right][\mathrm{J}_n(\varepsilon_{n,k})]^2, \tag{35}$$

$$\beta_{n,i,k} = \frac{1}{a^2}\int_0^a \mathrm{J}_n(\varepsilon_{n,k} r/a)\mathrm{J}_n(\lambda_{n,i} r/a)\, r\,\mathrm{d}r = \frac{\lambda_{n,i}}{\varepsilon_{n,k}^2 - \lambda_{n,i}^2}\mathrm{J}_n'(\lambda_{n,i})\mathrm{J}_n(\varepsilon_{n,k}), \tag{36}$$

$$\gamma_{n,i,k} = \frac{1}{a^2}\int_0^a \mathrm{J}_n(\varepsilon_{n,k} r/a)\,\mathrm{I}_n(\lambda_{n,i} r/a) r\,\mathrm{d}r = \frac{\lambda_{n,i}}{\varepsilon_{n,k}^2 + \lambda_{n,i}^2}\mathrm{I}_n'(\lambda_{n,i})\mathrm{J}_n(\varepsilon_{n,k}). \tag{37}$$

Hence, the reference kinetic energy $T^*_{F_2}$ of the fluid associated with symmetric modes of the end-plates is given by

$$T^*_{F_2} = \frac{1}{2}\rho_F \left[\int_0^{2\pi}\int_0^a (\phi^{(2)})_{x=L/2} w_T r \,\mathrm{d}r\mathrm{d}\theta + \int_0^{2\pi}\int_0^a (\phi^{(2)})_{x=-L/2} w_B r \,\mathrm{d}r\mathrm{d}\theta \right]$$

$$= \rho_F a^3 \psi_n \sum_{i=0}^{\infty}\sum_{h=0}^{\infty} b_i b_h \sum_{k=1}^{\infty} \frac{(A_{n,i}\beta_{n,i,k} + C_{n,i}\gamma_{n,i,k})}{\alpha_{n,k}\varepsilon_{n,k}} \frac{(A_{n,h}\beta_{n,h,k} + C_{n,h}\gamma_{n,h,k})}{\tanh(\varepsilon_{n,k}L/(2a))}. \quad (38)$$

For antisymmetric modes, equation (31) is replaced by

$$\Phi_i^{(2)}(x,r,\theta) = \begin{cases} K_{0,i,0}x + \sum_{k=1}^{\infty} K_{0,i,k} \mathrm{J}_0(\varepsilon_{0,k}r/a)\sinh(\varepsilon_{0,k}x/a) & \text{for } n = 0, \\ \cos(n\theta)\sum_{k=1}^{\infty} K_{n,i,k}\mathrm{J}_n(\varepsilon_{n,k}r/a)\sinh(\varepsilon_{n,k}x/a) & \text{for } n \neq 0. \end{cases} \quad (39)$$

The constants $K_{n,i,k}$ in this case are given by

$$K_{n,i,k} = -\frac{a(A_{n,i}\beta_{n,i,k} + C_{n,i}\gamma_{n,i,k})}{(\alpha_{n,k}\varepsilon_{n,k})\cosh(\varepsilon_{n,k}L/(2a))}. \quad (40)$$

In addition, the constant $K_{0,i,0}$ is given by

$$K_{0,i,0} = -2\tau_{0,i}, \quad (41)$$

where (Wheelon 1968)

$$\tau_{0,i} = \frac{1}{a^2}\int_0^a [A_{0,i}\mathrm{J}_0(\lambda_{0,i}r/a) + C_{0,i}\mathrm{I}_0(\lambda_{0,i}r/a)]\, r \,\mathrm{d}r = \left[\frac{A_{0,i}}{\lambda_{0,i}}\mathrm{J}_1(\lambda_{0,i}) + \frac{C_{0,i}}{\lambda_{0,i}}\mathrm{I}_1(\lambda_{0,i})\right]. \quad (42)$$

Hence, the reference kinetic energy $T^*_{F_2}$ of the fluid associated with antisymmetric modes of the end plates is given by

$$T^*_{F_2} = \begin{cases} \rho_F a^3 \psi_n \sum_{i=0}^{\infty}\sum_{h=0}^{\infty} b_i b_h \sum_{k=1}^{\infty} \frac{(A_{n,i}\beta_{n,i,k} + C_{n,i}\gamma_{n,i,k})}{\alpha_{n,k}\varepsilon_{n,k}} (A_{n,h}\beta_{n,h,k} + C_{n,h}\gamma_{n,h,k}) \tanh\left(\frac{\varepsilon_{n,k}L}{2a}\right), \\ \qquad\qquad\qquad\qquad\qquad\qquad\qquad\qquad\qquad\qquad\qquad\qquad n \neq 0 \\ \rho_F a^3 \psi_0 \sum_{i=0}^{\infty}\sum_{h=0}^{\infty} b_i b_h \left[\frac{L}{a}\tau_{0,i}\tau_{0,h} + \sum_{k=1}^{\infty} \frac{(A_{0,i}\beta_{0,i,k} + C_{0,i}\gamma_{0,i,k})}{\alpha_{0,k}\varepsilon_{0,k}} \right. \\ \left. \times (A_{0,h}\beta_{0,h,k} + C_{0,h}\gamma_{0,h,k}) \tanh\left(\frac{\varepsilon_{0,k}L}{2a}\right)\right], \\ \qquad\qquad\qquad\qquad\qquad\qquad\qquad\qquad\qquad\qquad\qquad\qquad n = 0. \end{cases} \quad (43)$$

3.3. Shell-Plate Interaction Via the Fluid

Equation (19) shows that in the reference kinetic energy of the fluid T^*_F, two terms appear because of the coupling effect of the fluid. In fact, even if the coupling springs between the plates and the shell were eliminated, the vibration of the two-end plates and the shell would remain coupled by the fluid inside the can. In particular, the quantity $T^*_{F_{1-2}}$, for symmetric

modes, is given by

$$T^*_{F_{1-2}} = -\frac{1}{2}\rho_F \int_0^{2\pi}\int_{-L/2}^{L/2} (\phi^{(2)})_{r=a}\, wa\,\mathrm{d}x\,\mathrm{d}\theta = -\frac{1}{2}\rho_F a\psi_n \sum_{s=1}^{\infty}\sum_{i=0}^{\infty} q_s b_i \sum_{k=1}^{\infty} K_{n,i,k}\mathrm{J}_n(\varepsilon_{n,k})\,\zeta^{(S)}_{n,s,k}, \tag{44}$$

where the constants $K_{n,i,k}$ are given by equation (34) and

$$\zeta^{(S)}_{n,s,k} = \int_{-L/2}^{L/2} \cos((2s-1)\pi x/L)\cosh(\varepsilon_{n,k}x/a)\,\mathrm{d}x = \frac{-2(2s-1)(-1)^s\pi a^2 L\cosh(\varepsilon_{n,k}L/(2a))}{(2s-1)^2\pi^2a^2 + L^2\varepsilon^2_{n,k}}. \tag{45}$$

The quantity $T^*_{F_{1-2}}$, for antisymmetric modes, is given by

$$T^*_{F_{1-2}} = \begin{cases} -\dfrac{1}{2}\rho_F a\psi_n \displaystyle\sum_{s=1}^{\infty}\sum_{i=0}^{\infty} q_s b_i \sum_{k=1}^{\infty} K_{n,i,k}\mathrm{J}_n(\varepsilon_{n,k})\,\zeta^{(A)}_{n,s,k}, & n \neq 0, \\ -\dfrac{1}{2}\rho_F a\psi_0 \displaystyle\sum_{s=1}^{\infty}\sum_{i=0}^{\infty} q_s b_i \left[-2\tau_{0,i}\zeta^{(A)}_{0,s} + \sum_{k=1}^{\infty} K_{0,i,k}\mathrm{J}_0(\varepsilon_{0,k})\,\zeta^{(A)}_{0,s,k}\right], & n = 0, \end{cases} \tag{46}$$

where the constants $K_{n,i,k}$ are given by equation (40) and

$$\zeta^{(A)}_{0,s} = \int_{-L/2}^{L/2} x\sin(2s\pi x/L)\,\mathrm{d}x = \frac{-(-1)^s L^2}{2s\pi}, \tag{47}$$

$$\zeta^{(A)}_{n,s,k} = \int_{-L/2}^{L/2} \sin(2s\pi x/L)\sinh(\varepsilon_{n,k}x/a)\,\mathrm{d}x = \frac{-4s(-1)^s\pi a^2 L\sinh(\varepsilon_{n,k}L/(2a))}{4s^2\pi^2a^2 + L^2\varepsilon^2_{n,k}}. \tag{48}$$

The component $T^*_{F_{2-1}}$ of the reference kinetic energy of the fluid has the following expression for symmetric modes:

$$\begin{aligned} T^*_{F_{2-1}} &= \frac{1}{2}\rho_F\left[\int_0^{2\pi}\int_0^{a} (\phi^{(1)})_{x=-L/2} w_B r\,\mathrm{d}r\,\mathrm{d}\theta + \int_0^{2\pi}\int_0^{a} (\phi^{(1)})_{x=L/2} w_T r\,\mathrm{d}r\,\mathrm{d}\theta\right] \\ &= -\frac{1}{\pi}\rho_F\psi_n \sum_{s=1}^{\infty}\sum_{i=0}^{\infty} q_s b_i \left[\frac{-2(-1)^s a^3}{(2s-1)n\lambda_{n,i}}(A_{n,i}\mathrm{J}_{n+1}(\lambda_{n,i}) + C_{n,i}\mathrm{I}_{n+1}(\lambda_{n,i})) \right. \\ &\quad \left. + \sum_{m=1}^{\infty}\frac{(-1)^m\sigma^{(S)}_{s,m}}{m\mathrm{I}'_n(2m\pi a/L)}(A_{n,i}\xi^{(S)}_{n,i,m} + C_{n,i}\mu^{(S)}_{n,i,m})\right], \end{aligned} \tag{49}$$

where the constants $\sigma^{(S)}_{s,m}$ are given in equation (24), and (Wheelon 1968)

$$\begin{aligned} \xi^{(S)}_{n,i,m} &= \int_0^{a} \mathrm{I}_n(2m\pi r/L)\mathrm{J}_n(\lambda_{n,i}r/a)r\,\mathrm{d}r \\ &= \frac{2m\pi a^3 L\mathrm{I}_{n+1}(2m\pi a/L)\mathrm{J}_n(\lambda_{n,i}) + a^2L^2\lambda_{n,i}\mathrm{I}_n(2m\pi a/L)\mathrm{J}_{n+1}(\lambda_{n,i})}{4m^2\pi^2a^2 + L^2\lambda^2_{n,i}}, \end{aligned} \tag{50}$$

$$\begin{aligned} \mu^{(S)}_{n,i,m} &= \int_0^{a} \mathrm{I}_n(2m\pi r/L)\mathrm{I}_n(\lambda_{n,i}r/a)r\,\mathrm{d}r \\ &= \frac{2m\pi a^3 L\mathrm{I}_{n+1}(2m\pi a/L)\mathrm{I}_n(\lambda_{n,i}) - a^2L^2\lambda_{n,i}\mathrm{I}_n(2m\pi a/L)\mathrm{I}_{n+1}(\lambda_{n,i})}{4m^2\pi^2a^2 - L^2\lambda^2_{n,i}}. \end{aligned} \tag{51}$$

The term $T^*_{F_{2-1}}$ for antisymmetric modes is given by

$$T^*_{F_{2-1}} = -\frac{2}{\pi}\rho_F \psi_n \sum_{s=1}^{\infty}\sum_{i=0}^{\infty} q_s b_i \sum_{m=1}^{\infty} \frac{(-1)^m \sigma^{(A)}_{s,m}}{(2m-1)\mathrm{I}'_n((2m-1)\pi a/L)}(A_{n,i}\xi^{(A)}_{n,i,m} + C_{n,i}\mu^{(A)}_{n,i,m}), \quad (52)$$

where the constants $\sigma^{(A)}_{s,m}$ are given in equation (28); $\xi^{(A)}_{n,i,m}$ and $\mu^{(A)}_{n,i,m}$ are obtained replacing $2m$ by $(2m\text{-}1)$ in equations (50) and (51), respectively.

3.4. Symmetric Modes for $n = 0$ and fluid Volume Conservation

In the case of symmetric modes and $n = 0$ the condition for the conservation of the volume of the contained incompressible fluid must be imposed; in all the other cases it is automatically satisfied by the assumed mode shapes. It is given by

$$\sum_{s=1}^{\infty} q_s \int_0^{2\pi}\int_{-L/2}^{L/2} \cos((2s-1)\pi x/L)a\,\mathrm{d}x\,\mathrm{d}\theta = 2\sum_{i=0}^{\infty} b_i \int_0^{2\pi}\int_0^{a} [A_{0,i}\mathrm{J}_0(\lambda_{0,i}r/a) + C_{0,i}\mathrm{I}_0(\lambda_{0,i}r/a)]\,r\,\mathrm{d}r\,\mathrm{d}\theta. \quad (53)$$

After simple calculations, one obtains

$$-(L/\pi)\sum_{s=1}^{\infty} q_s(-1)^s/(2s-1) = a\sum_{i=0}^{\infty} b_i \tau_{0,i}. \quad (54)$$

For symmetric modes and $n = 0$ two additional terms must be added to the fluid deformation potential ϕ previously calculated. The first term is the constant ϕ_0 that gives an additional contribution to the reference kinetic energy of the fluid,

$$\rho_F a(L/\pi)\psi_0\phi_0\sum_{s=1}^{\infty} q_s(-1)^s/(2s-1) + \rho_F a^2\psi_0\phi_0\sum_{i=0}^{\infty} b_i\tau_{0,i}. \quad (55)$$

By using equation (54) it is found that this contribution must be zero.

The second additional term is ϕ_a and is given by

$$\phi_a = c_0(r^2 - 2x^2), \quad (56)$$

where c_0 must satisfy the condition of contact with a flexible wall

$$(\partial\phi_a/\partial r)_{r=a} = 2ac_0 = -(1/L)\sum_{s=1}^{\infty} q_s \int_{-L/2}^{L/2} \cos[(2s-1)\pi x/L]\mathrm{d}x \quad (57)$$

and

$$(\partial\phi_a/\partial x)_{x=L/2} = -2Lc_0 = (2/a^2)\sum_{i=0}^{\infty} b_i \int_0^{a} [A_{0,i}\mathrm{J}_0(\lambda_{0,i}r/a) + C_{0,i}\mathrm{I}_0(\lambda_{0,i}r/a)]r\,\mathrm{d}r. \quad (58)$$

From equations (57) and (58) we obtain, respectively,

$$c_0 = [1/(a\pi)]\sum_{s=1}^{\infty} q_s(-1)^s/(2s-1), \qquad c_0 = -(1/L)\sum_{i=0}^{\infty} b_i\tau_{0,i}. \quad (59a, b)$$

By using equation (54), we find that the right-hand side of equations (59a) and (59b) are equal; this result guarantees that ϕ_a is effectively a solution of our problem. The term ϕ_a is

associated with an additional reference kinetic energy given by

$$\rho_F \psi_0 \left\{ \frac{1}{\pi} \sum_{s=1}^{\infty} \sum_{j=1}^{\infty} q_s q_j \frac{(-1)^s}{2s-1} \left[\frac{(-1)^j a^2 L}{(2j-1)\pi} + \tilde{\alpha}_{0,j} \right] - \frac{1}{L} \sum_{i=0}^{\infty} \sum_{h=0}^{\infty} b_i b_h \tau_{0,i} \left[\tilde{\beta}_{0,h} - \frac{L^2 a^2}{2} \tau_{0,h} \right] \right\}, \tag{60}$$

where

$$\tilde{\alpha}_{0,j} = \int_{-L/2}^{L/2} x^2 \cos\left[(2j-1)\pi x/L\right] \mathrm{d}x = \frac{L^3 (8 - \pi^2 + 4\pi^2 j - 4\pi^2 j^2)(-1)^j}{2\pi^3 (2j-1)^3} \tag{61}$$

and

$$\tilde{\beta}_{0,h} = \int_0^a r^3 \left[A_{0,h} \mathrm{J}_0(\lambda_{0,h} r/a) + C_{0,h} \mathrm{I}_0(\lambda_{0,h} r/a) \right] \mathrm{d}r = (a^4/\lambda_{0,h}^2) \{ A_{0,h} [2\mathrm{J}_2(\lambda_{0,h}) - \lambda_{0,h} \mathrm{J}_3(\lambda_{0,h})]$$
$$+ C_{0,h} [2\mathrm{I}_2(\lambda_{0,h}) + \lambda_{0,h} \mathrm{I}_3(\lambda_{0,h})] \}. \tag{62}$$

4. THE RAYLEIGH–RITZ METHOD

In order to solve the problem, it is useful to introduce the Rayleigh quotient (Amabili 1997b; Zhu 1994) for the systems considered, which is

$$\omega^2 = (V_S + V_P + V_C)/(T_S^* + T_P^* + T_F^*). \tag{63}$$

For the numerical calculation of the natural frequencies and the parameters of the Ritz expansion of modes, only N terms in the expansion of w, equation (1), and $\bar{N}$ in the expansion of w_B and w_T, equations (2) and (3), are considered, where N and $\bar{N}$ must be chosen large enough to give the required accuracy to the solution. Thus, all the energies are given by finite summations. Here it is convenient to introduce a vectorial notation. The vector $\mathbf{q}$ of the parameters of the Ritz expansions is defined by

$$\mathbf{q}^{\mathrm{T}} = \{\{q\}^{\mathrm{T}}, \{b\}^{\mathrm{T}}\}, \quad \{q\}^{\mathrm{T}} = \{q_1, \ldots q_N\}, \quad \{b\}^{\mathrm{T}} = \{b_0, \ldots, \mathrm{b}_{\bar{N}-1}\}. \tag{64a–c}$$

Maximum potential energies V_S, V_P and V_C and reference kinetic energies T_S^*, T_P^* and T_F^* can be written in the following form:

$$T_{\#}^* = \mathbf{q}^{\mathrm{T}} \mathbf{M}_{\#} \mathbf{q}, \qquad V_{\#} = \mathbf{q}^{\mathrm{T}} \mathbf{K}_{\#} \mathbf{q}, \tag{65a, b}$$

where $\mathbf{M}_{\#}$ and $\mathbf{K}_{\#}$ are $(N+\bar{N}) \times (N+\bar{N})$ matrices and $\#$ replaces the symbols S, P and F in equation (65a) and S, P and C in equation (65b). Thus, the values of the vector $\mathbf{q}$ of the Ritz parameters are determined in order to render equation (63) stationary, and the following Galerkin equation is obtained:

$$(\mathbf{K}_S + \mathbf{K}_P + \mathbf{K}_C)\mathbf{q} - \omega^2 (\mathbf{M}_S + \mathbf{M}_P + \mathbf{M}_F)\mathbf{q} = \mathbf{0}, \tag{66}$$

where ω is the circular frequency (rad/s) of the fluid-filled hermetic can. Equation (66) gives a linear eigenvalue problem for a real, symmetric matrix; real eigenvalues are obtained.

In the case of symmetric modes, for $n = 0$ the Galerkin equation is

$$\left[\begin{array}{c|c} \mathbf{K}_S + \mathbf{K}_P + \mathbf{K}_C & \mathbf{0} \\ \hline \mathbf{0}^{\mathrm{T}} & 0 \end{array}\right] \left\{\begin{array}{c} \mathbf{q} \\ \hline \phi_0 \end{array}\right\} - \omega^2 \left[\begin{array}{c|c} \mathbf{M}_S + \mathbf{M}_P + \mathbf{M}_F & \mathbf{M}_A \\ \hline \mathbf{M}_A^{\mathrm{T}} & 0 \end{array}\right] \left\{\begin{array}{c} \mathbf{q} \\ \hline \phi_0 \end{array}\right\} = \mathbf{0}, \tag{67}$$

TABLE 1

Comparison of natural frequencies (Hz) computed for the studied empty can and $n = 3$; S and P indicate shell- and plate-dominant modes, respectively

Mode	Present study		Huang & Soedel (1993)	Difference (%)
Symmetric	1st (S)	1734	1735	0·06
	2nd (P)	2384	2343	1·7
	3rd (P)	5124	5080	0·86
	4th (S)	6003	5997	0·1
Antisymmetric	1st (P)	2365	2326	1·6
	2nd (S)	4223	4224	0·02
	3rd (P)	5177	5125	1·0
	4th (S)	7100	7102	0·03

where the vector $\mathbf{M}_A$ has dimension $(N + \bar{N})$ and represents the additional term to the reference kinetic energy of the fluid given by equation (55) that must be zero; the last row in equation (67) expresses the conservation of the fluid volume. Matrix $\mathbf{M}_F$ includes the contribution of equation (60) in this case. The first eigenvalue of equation (67) is zero; it corresponds to $\mathbf{q} = \mathbf{0}$ and must be disregarded.

In addition, the pressure exerted by the fluid at a point of the can wall can be computed by using the linearized Bernoulli equation

$$(p)_{\text{point}} = \rho_F(\partial\tilde{\phi}/\partial t)_{\text{point}} = -\rho_F\omega^2(\phi)_{\text{point}}\,e^{i\omega t}. \tag{68}$$

5. NUMERICAL RESULTS AND DISCUSSION

Numerical results have been carried out by means of the *Mathematica* software (Wolfram 1996). The following dimensions and material properties have been chosen in order to compare the results with those obtained by Huang & Soedel (1993) in the case of an empty can: mean radius $a = 0{\cdot}1$ m, $L = 0{\cdot}2$ m, $h_S = h_P = 0{\cdot}002$ m, $E_S = E_P = 206 \times 10^9$ Pa, $\rho_S = \rho_P = 7850\ \text{kg/m}^3$ and $\nu_S = \nu_P = 0{\cdot}3$. Twenty shell and plate modes have been considered in the Rayleigh–Ritz expansions, and 20 terms have been included in the expansion of $\Phi_s^{(1)}$ and $\Phi_i^{(2)}$. They are enough to give a good accuracy, as will be shown in Section 5.2. The Flügge theory of shells has been used, unless otherwise specified.

The plate and the shell are assumed to be joined by rotational springs of very high stiffness c simulating a rigid joint. In the present case, it was found that a value of $c = 10^8$ N is enough to simulate a rigid rotational joint; in fact, an increment to this value does not affect the natural frequencies of the system. The effect of the joint flexibility on natural frequencies will be investigated in Section 5.2.

5.1. EMPTY CAN

This case has been analysed in order to compare the present results with data available in the literature. The comparison is shown in Table 1 for modes having $n = 3$ nodal diameters. A very good agreement between the natural frequencies obtained by Huang & Soedel (1993), who used the receptance method, and the present results was found.

It is interesting that, even though a completely flexible structure is studied, it is still possible to recognize modes dominated by the plate displacement (P mode) or by the shell displacement (S mode). Discussion on symmetric and antisymmetric modes with respect to

TABLE 2

Convergence of natural frequencies (Hz) with the number of terms $N = \bar{N}$ in the expansion of mode shapes for the studied water-filled can and $n = 3$; S and P indicate shell and plate-dominant modes, respectively

Mode		$N = 10$	$N = 15$	$N = 20$	$N = 25$	$N = 30$
Symmetric	1st (S)	1013	1012	1011	1011	1011
	2nd (P)	1685	1653	1638	1629	1623
	3rd (S)	3922	3918	3914	3909	3905
	4th (P)	4074	4005	3977	3964	3956
Antisymmetric	1st (P)	1683	1652	1637	1628	1623
	2nd (S)	2607	2603	2601	2600	2600
	3rd (P)	4061	4003	3976	3960	3951
	4th (S)	4981	4964	4957	4952	4950

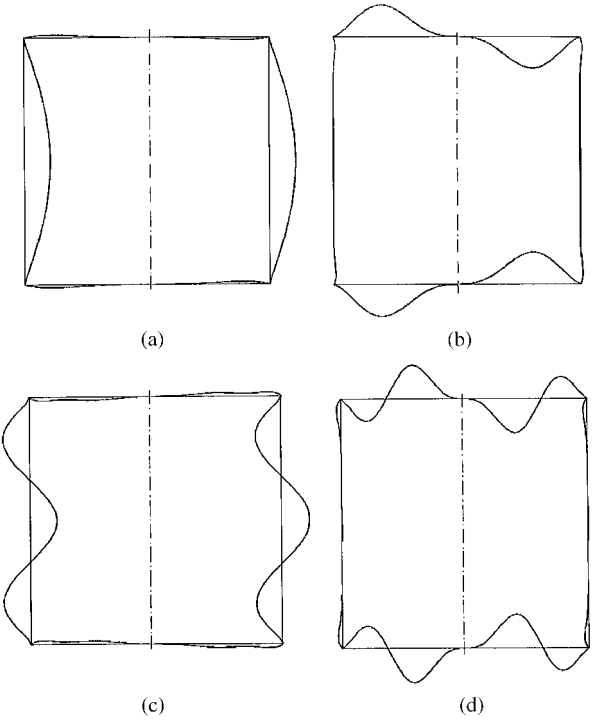

Figure 2. First four symmetric modes of the can filled with water; $n = 3$: (a) 1st S mode, 1011 Hz; (b) 1st P mode, 1638 Hz; (c) 2nd S mode, 3914 Hz; (d) 2nd P mode, 3977 Hz.

plane $x = 0$ has been made in the previous sections. However, it can still be observed that, when n is odd and one observes a can section along its axis, one gets antisymmetric mode shapes with respect to the can axis; while, for n even, one gets symmetric shapes.

5.2. WATER-FILLED CAN

The can is assumed to be completely filled with water having a mass density $\rho_F = 1000\ \text{kg/m}^3$. Table 2 shows the convergence of the method as the number of terms in

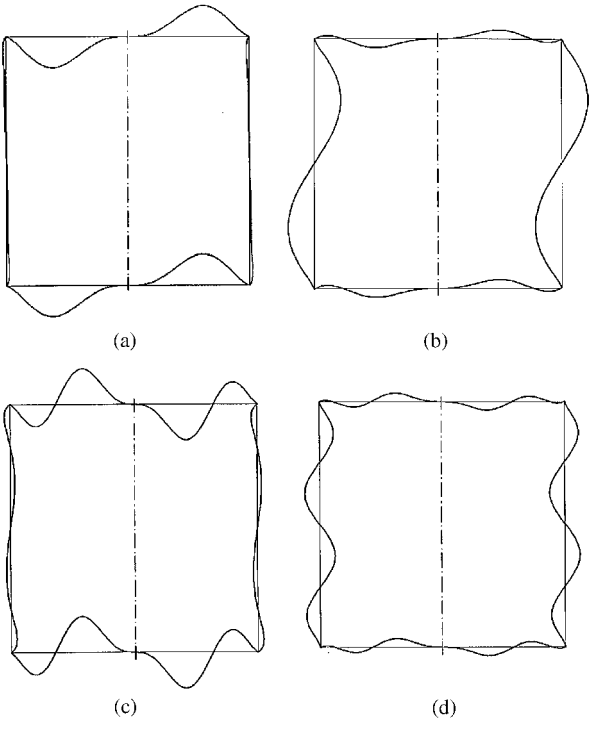

Figure 3. First four antisymmetric modes of the can filled with water; $n = 3$. (a) 1st P mode, 1637 Hz; (b) 1st S mode, 2601 Hz; (c) 2nd P mode, 3976 Hz; (d) 2nd S mode, 4957 Hz.

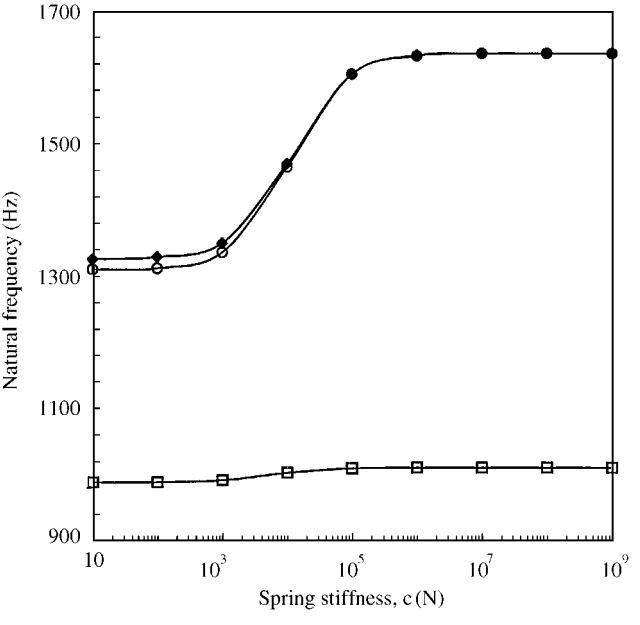

Figure 4. Effect of spring stiffness c on natural frequencies of the water-filled can; $n = 3$: ⊟, 1st S mode (symmetric); ◆, 1st P mode (symmetric); ○, 1st P mode (antisymmetric:)

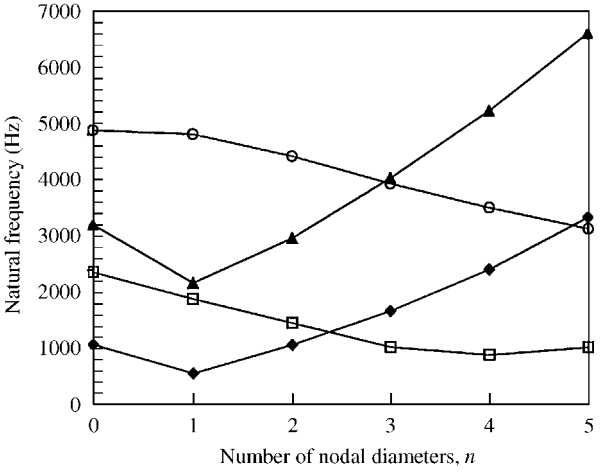

Figure 5. Natural frequencies of symmetric modes versus the number of nodal diameters; water-filled can: ◆, 1st P mode; □, 1st S mode; ▲, 2nd P mode; ○, 2nd S mode.

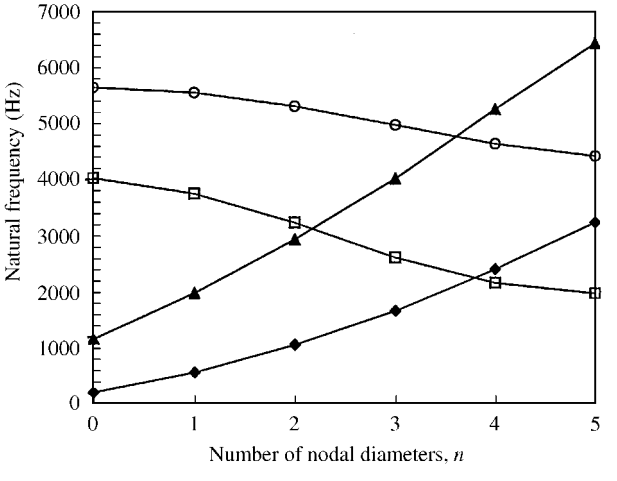

Figure 6. Natural frequencies of antisymmetric modes versus the number of nodal diameters; water-filled can: ◆, 1st P mode; □, 1st S mode; ▲, 2nd P mode; ○, 2nd S mode.

the series expansions is increased; it is seen that 20 terms give good accuracy for this application. It was also observed that the first shell-dominant mode converges very quickly for both symmetric and antisymmetric cases. The third symmetric mode (shell-dominant) converges slowly as a consequence of its mode shape involving many plate modes; however, the difference between the natural frequency evaluated with 10 terms and the one evaluated with 30 terms is of 0·4% only. In general, more terms are necessary to estimate with good accuracy the natural frequencies of plate-dominant modes.

Figure 2 shows symmetric modes of the water-filled can for $n = 3$. Natural frequencies are given in the caption and show a large reduction with respect to the empty case. The first and third modes are shell-dominant, while the second and fourth modes are plate-dominant. Figure 3 shows antisymmetric modes for the same case. In this case, the first and third

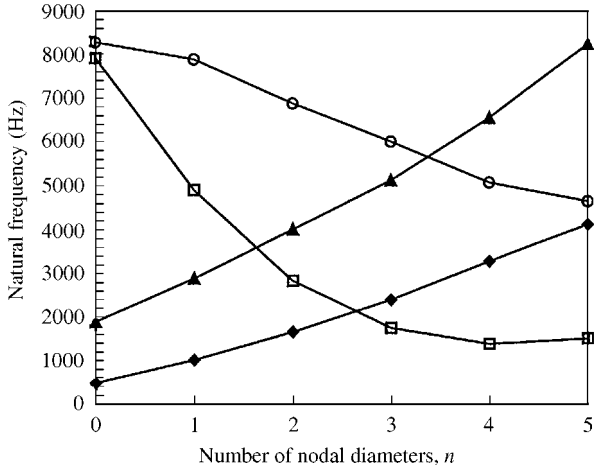

Figure 7. Natural frequencies of symmetric modes versus the number of nodal diameters; empty can: ◆, 1st P mode; □, 1st S mode; ▲, 2nd P mode; ○, 2nd S mode.

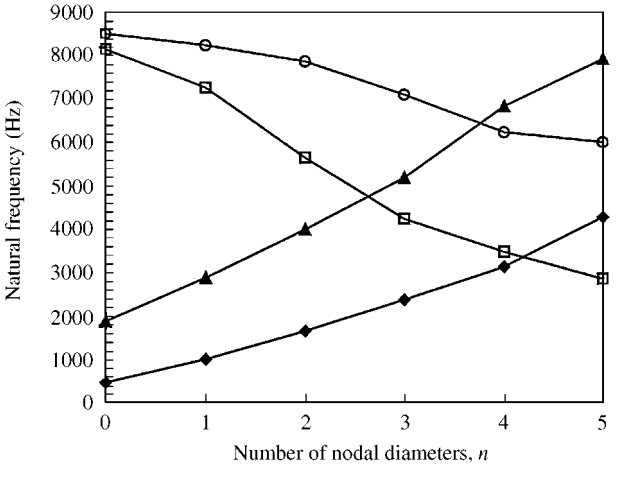

Figure 8. Natural frequencies of antisymmetric modes versus the number of nodal diameters; empty can: ◆, 1st P mode; □, 1st S mode; ▲, 2nd P mode; ○, 2nd S mode.

modes are plate-dominant, while the second and fourth are shell-dominant. The fourth mode is particularly interesting because it shows a large interaction of shell and plates in the dynamic behaviour of the system.

The effect of the stiffness of the joint at the shell–plate junctions is investigated in Figure 4. Here it is seen that all curves become horizontal for $c = 10^7$ N; therefore a further increase of the joint stiffness over this value does not affect natural frequencies. For the case studied, the values of joint stiffness having the largest influence on natural modes lie between 10^3 and 10^5 N.

Natural frequencies of symmetric and antisymmetric modes computed for different numbers of nodal diameters n are given in Figures 5 and 6, respectively. Natural frequencies of plate-dominant modes increase with n, excluding the case $n = 0$ of symmetric modes that has a particular behaviour, as already described in previous sections. In fact, this case is

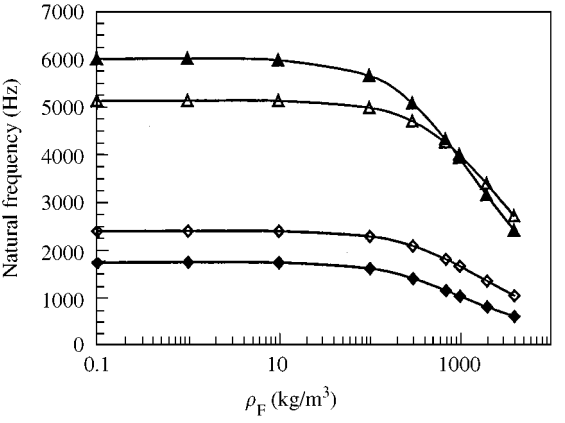

Figure 9. Natural frequencies of the first four symmetric modes of the can versus the fluid density; $n = 3$: —◆—1st S mode; —◇—, 1st P mode; —▲— 2nd S mode; —△— 2nd P mode.

governed by volume conservation, so that the plate mode without nodal circles is impossible and the first plate mode has one nodal circle. Natural frequencies of shell-dominant modes initially decrease with n, and then increase. In particular, the first shell-dominant symmetric mode has its minimum natural frequency for $n = 4$. Figures 5 and 6 can be compared to the analogous Figures 7 and 8 obtained for the same empty can (with vacuum inside; in case of air inside, it is necessary to include the acoustic modes of the cavity) in order to evaluate the effect of the water contained.

The effect of the density of the contained fluid on the natural frequencies of the first two shell- and plate-dominant symmetric modes with $n = 3$ is shown in Figure 9. In particular, the 2nd shell-dominant mode is more sensible to the increment of the fluid density than the 2nd plate-dominant mode; therefore, for $\rho_F \cong 1000$ kg/m^3 the 2nd shell-dominant mode is associated with a frequency lower than that of the 2nd plate-dominant mode.

The relative edge stiffness of the coupled shell and plates is fundamental to having a strong interaction between shell and plate modes. Figure 10 shows the effect of the thickness of the end-plates on the natural frequencies of the system for symmetric modes with $n = 3$. In particular, the effect of the plate thickness on the first shell-dominant mode is given in Figure 10(a) and the effect on the first two plate-dominant modes is presented in Figure 10(b). Figure 10(a) shows that the natural frequency of the first shell-dominant mode changes significantly for a plate thickness lying between 1 and 8 mm; outside this interval, its change is much less significant. In fact, very thin end-plates cannot constrain shell rotation at the edge and give a constraint to the shell that is very close to a simple support; on the other hand, very thick end-plates give a constraint to the shell that is very close to clamped edges.

The proposed method is suitable for the study of two plates in a rigid cylindrical container and of a shell closed by two rigid ends in the presence of dense fluid. The last case is particularly interesting because it allows comparison with the classical, and much simpler, problem of a simply supported shell with open ends ($\phi = 0$ for $x = \pm L/2$) completely filled with water. Comparison is presented in Table 3 for a simply supported shell having the same material properties as the previously studied can and dimensions: $a = 0{\cdot}175$ m, $L = 0{\cdot}6$ m and $h_S = 0{\cdot}001$ m. Natural frequencies of a shell with closed ends are always smaller than those of a shell with open ends. This is due to the larger added mass of the contained water that increases when the liquid is more constrained, as observed in other fluid–structure systems (Amabili & Kwak 1996). Differences for the shell studied with open

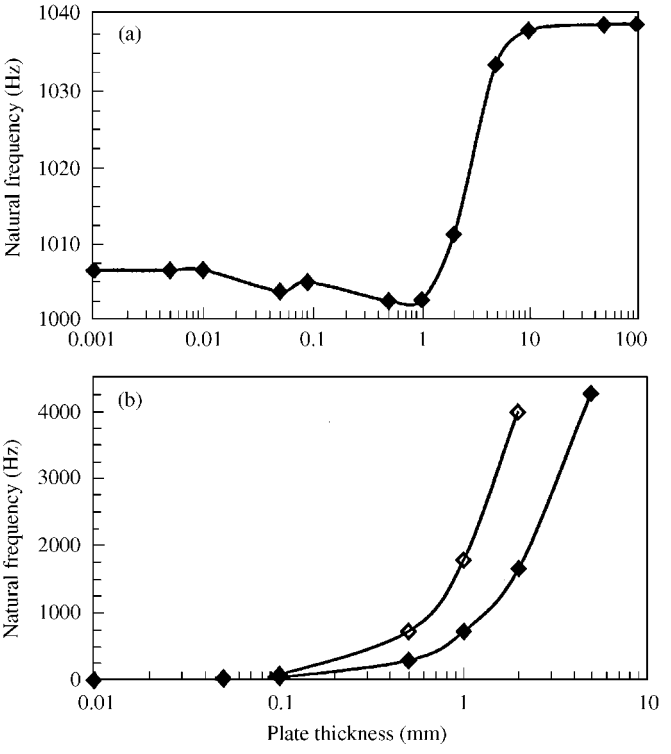

Figure 10. Natural frequencies of symmetric modes of the water-filled can versus the plate thickness; $n = 3$. (a) 1st S mode; (b) —◆—, 1st P mode; —◇—, 2nd P mode.

TABLE 3
Natural frequencies (Hz) of the simply supported shell with closed and open ends filled with water (Donnell's theory of shells) for $n = 4$

m	Closed ends	Open ends	Difference (%)
1	102·3	105·3	2·9
2	318·8	330·0	3·5
3	602·7	625·9	3·8
4	892·3	927·3	3·9
5	1160·2	1205·5	3·9
6	1398·8	1452·5	3·8
7	1609·9	1669·7	3·7
8	1798·2	1861·4	3·5

and closed ends lie between 2·9 and 3·9% for the modes considered. It is of interest to observe that the condition of rigid end-plates can be obtained by the present theory by giving a very high value to Young's modulus of the plates ($E_P \to \infty$).

6. CONCLUSIONS

Natural modes of cans are largely affected by the presence of a dense fluid inside. In fact, for lower modes, the fluid pressure on the wetted surface is in phase with the structural

acceleration, thus the fluid appears as an added mass. However, for symmetric modes and $n = 0$, the fluid volume conservation plays an important role, so that plate modes without nodal circles are no longer possible. Shell- and plate-dominant modes are still recognizable for the first modes and different n values; however, already the first modes present an important interaction of shell and plate modes. This phenomenon is magnified when the flexural rigidity of shell and plates is similar (for the usual geometry, when the shell is thinner than the plates). The effect of the joint flexibility at the shell-plate links can be very large and the full range of flexibility has been investigated.

The special case of a flexible, water-filled shell closed by rigid ends displays natural frequencies larger by a few present than the same water-filled shell with open ends; in fact, constraints to the fluid movement enhance the added mass of the contained fluid.

ACKNOWLEDGEMENTS

This research was partially supported by the Italian Space Agency (ASI).

References

Amabili, M. 1997a Shell-plate interaction in the free vibrations of circular cylindrical tanks partially filled with a liquid: the artificial spring method. *Journal of Sound and Vibration* **199,** 431–452.

Amabili, M. 1997b Ritz method and substructuring in the study of vibration with strong fluid-structure interaction. *Journal of Fluids and Structures* **11,** 507–523.

Amabili, M. 1997c Bulging modes of circular bottom plates in rigid cylindrical containers filled with a liquid. *Shock and Vibration* **4,** 51–68.

Amabili, M. & Dalpiaz, G. 1995 Breathing vibrations of a horizontal circular cylindrical tank shell, partially filled with liquid. *ASME Journal of Vibration and Acoustics* **117,** 187–191.

Amabili, M. & Kwak, M. K. 1996 Free vibrations of circular plates coupled with liquids: revising the Lamb problem. *Journal of Fluids and Structures* **10,** 743–761.

Amabili, M., Païdoussis, M. P. & Lakis, A. A. 1998 Vibrations of partially filled cylindrical tanks with ring-stiffeners and flexible bottom. *Journal of Sound and Vibration* **213,** 259–299.

Bauer, H. F. 1995 Coupled frequencies of a liquid in a circular cylindrical container with elastic liquid surface cover. *Journal of Sound and Vibration* **180,** 689–704.

Bauer, H. F. & Siekmann, J. 1971 Dynamic interaction of a liquid with the elastic structure of a circular cylindrical container. *Ingenieur Archiv* **40,** 266–280.

Berry, J. G. & Reissner, E. 1958 The effect of an internal compressible fluid column on the breathing vibrations of a thin pressurized cylindrical shell. *Journal of Aeronautical Science* **25,** 288–294.

Bhuta, G. & Koval, L. R. 1964 Hydroelastic solution of the sloshing of a liquid in a cylindrical tank. *Journal of the Acoustical Society of America* **36,** 2071–2079.

Cheng, L. 1994 Fluid-structural coupling of a plate-ended cylindrical shell: vibration and internal sound field. *Journal of Sound and Vibration* **174,** 641–654.

Cheng, L. & Nicolas, J. 1992 Free vibration analysis of a cylindrical shell-circular plate system with general coupling and various boundary conditions. *Journal of Sound and Vibration* **155,** 231–247.

Chiba, M. 1993 Nonlinear hydroelastic vibration of a cylindrical tank with an elastic bottom, containing liquid. Part II: Linear axisymmetric vibration analysis. *Journal of Fluids and Structures* **7,** 57–73.

Chiba, M. 1996 Free vibration of a partially liquid-filled and partially submerged, clamped-free circular cylindrical shell. *Journal of the Acoustical Society of America* **100,** 2170–2180.

Gonçalves, P. B. & Ramos, N. R. S. S. 1996 Free vibration analysis of cylindrical tanks partially filled with liquid. *Journal of Sound and Vibration* **195,** 429–444.

Harari, A., Sandman, B., & Zaldonis, J. A. 1994 Analytical and experimental determination of the vibration and pressure radiation from a submerged, stiffened cylindrical shell with two end plates. *Journal of the Acoustical Society of America* **95,** 3360–3368.

Hirano, Y. 1969 Axisymmetric vibrations of thin drums. *Bulletin of the Japan Society of Mechanical Engineers* **12,** 459–469.

Huang, D. T. & Soedel, W. 1993 On the free vibrations of multiple plates welded to a cylindrical shell with special attention to mode pairs. *Journal of Sound and Vibration* **166,** 315–339.

LAKIS, A. A. & PAÏDOUSSIS, M. P. 1971 Free vibration of cylindrical shells partially filled with liquid. *Journal of Sound and Vibration* **19,** 1–15.

LEISSA, A. W. 1973 *Vibration of Shells*, NASA SP-288. Washington DC: Government Printing Office. Now available from The Acoustical Society of America (1993).

LEISSA, A. W. & NARITA, Y. 1980 Natural frequencies of simply supported circular plates. *Journal of Sound and Vibration* **70,** 221–229.

TAKAHASHI, S. & HIRANO, Y. 1970 Vibration of a combination of circular plates and cylindrical shells (first report, A cylindrical shell with circular plates at ends). *Bulletin of the Japan Society of Mechanical Engineers* **13,** 240–247.

TAVAKOLI, M. S. & SINGH, R. 1989 Eigensolutions of joined/hermetic shell structures using the state space method. *Journal of Sound and Vibration* **100,** 97–123.

TAVAKOLI, M. S. & SINGH, R. 1990 Modal analysis of a hermetic can. *Journal of Sound and Vibration* **136,** 141–145.

WHEELON, A. D. 1968 *Tables of Summable Series and Integrals Involving Bessel Functions*. San Francisco, CA: Holden-Day.

WOLFRAM, S. 1996 *The Mathematica Book*, 3rd edition. Cambridge, UK: Cambridge University Press.

YAMAKI, N., TANI, J. & YAMAJI, T. 1984 Free vibration of a clamped-clamped circular cylindrical shell partially filled with liquid. *Journal of Sound and Vibration* **94,** 531–550.

YUAN, J. & DICKINSON, S. M. 1992 On the use of artificial springs in the study of the free vibrations of systems comprised of straight and curved beams. *Journal of Sound and Vibration* **153,** 203–216.

YUAN, J. & DICKINSON, S. M. 1994 The free vibration of circularly cylindrical shell and plate systems. *Journal of Sound and Vibration* **175,** 241–263.

ZHU, F. 1994 Rayleigh quotients for coupled free vibrations. *Journal of Sound and Vibration* **171,** 641–649.